

Characteristics of self-guided laser plasma channels generated by femtosecond laser pulses in air

Hui Yang, Jie Zhang,* Yingjun Li, Jun Zhang, Yutong Li, Zhenglin Chen, Hao Teng, Zhiyi Wei, and Zhengming Sheng
 Laboratory of Optical Physics, Institute of Physics, Chinese Academy of Sciences, Beijing 100080, China
 (Received 30 August 2001; revised manuscript received 21 March 2002; published 29 July 2002)

With ultrashort laser pulses (25 fs) and low energy ($E=15$ mJ), we observe laser plasma channels with a length over 5 m in air. The diameter of the plasma channel is measured to be $120\text{ }\mu\text{m}$. The average electron density in the channel is inferred to be about 10^{18} W/cm^3 with an interferometric method. At the same time, the temporal evolution of the electron density in the plasma channel is investigated. The resistivity in the plasma channel is measured to be less than $1\text{ }\Omega\text{ cm}$. It is suggested that the lifetime of the plasma channel can be greatly prolonged by launching another long laser pulse along the plasma channel.

DOI: 10.1103/PhysRevE.66.016406

PACS number(s): 52.35.Mw, 52.40.Db

I. INTRODUCTION

There is a great interest in understanding the propagation process of femtosecond laser pulses through air [1–9]. In 1996, Braun *et al.* [1] observed self-focusing into filaments in air with infrared laser pulses. The filaments can persist over several tens of meters. The mechanism for femtosecond laser pulses propagating over long distance in air is the balance between the Kerr self-focusing due to the nonlinear effects in air and defocusing due to the tunneling ionization and diffraction of the laser beam [6].

In this paper, we present our investigations on characteristics of plasma channels in air generated by femtosecond laser pulses. With an interferometric method, the initial average electron density in the channel is measured to be about 10^{18} cm^{-3} . The resistivity of the channel is found to be less than $1\text{ }\Omega\text{ cm}$. A plasma channel with a length longer than 5 m is observed and the channel diameter is measured to be about $120\text{ }\mu\text{m}$.

II. EXPERIMENTAL SETUP

In our experiments, femtosecond laser pulses were slightly focused with a positive lens ($f=40$ cm, 2 m, 4 m) in air. At the same time, with an interferometric method as shown in Fig. 1, the electron density in the plasma channel was measured. The laser system is a home-made Ti:sapphire laser system, that can provide up to 45 mJ energy, in 25 fs pulses, at a central wavelength of 800 nm. The laser beam was focused in air and formed a plasma channel. A small portion of the laser beam was frequency doubled by a BBO crystal to serve as a probing laser beam. The delay between the main laser beam and the probing laser beam could be adjusted. After transmitting through the plasma channel, the probing beam was focused through a Wollaston prism and a polarizer. Finally the interferometric fringes were recorded by a charge-coupled device (CCD) camera. At the same time, we measured the length and diameter of the plasma channel with a CCD camera (512×512 pixels) with a pixel size of $24\text{ }\mu\text{m}$.

III. RESULTS AND ANALYSIS

A typical image of the plasma channel is shown in Fig. 2, where a lens with $f=2$ m was used to slightly focus the laser beam. Generally the length of the channel varied with the focus length of the lens. The length of the channel was about 30 cm when using a lens of $f=1.5$ m. It became longer than 50 cm as shown in Fig. 2(a), when a lens of $f=2$ m was used. Furthermore, when a lens with $f=4$ m was used, a good conductive plasma channel with a length greater than 5 m was observed. From Fig. 2(b), we can find that the laser intensity distribution in the channel is close to a Gaussian and the Gaussian-fitting diameter of the filament is about $120\text{ }\mu\text{m}$. The Rayleigh length of the laser beam is about 14 mm for this diameter. We then know that the laser beam can propagate over hundred Rayleigh lengths. This result is in good agreement with our calculations [6].

An analysis shows that the electron distribution initially created by the laser pulse can be very quickly smoothed by recombination and collisional processes. To measure the electron density in the channel, we used an interferometric method as shown in Fig. 1 [12]. Because the laser intensity in the channel is only about 10^{14} W/cm^2 , the static magnetic field can be omitted. The refractive index in air therefore can be expressed as

$$N^2 = 1 - \omega_p^2 / \omega_L^2, \quad (1)$$

where N is the refractive index of the plasma channel, ω_p is the plasma frequency, and ω_L is the laser frequency. When the probing beam traverses the plasmas channel, the phase-shifted probing beam can be written as

$$\Delta\Phi = \int (k_p - k_0) dl = \int (N - 1) \omega / c dl, \quad (2)$$

where $k_0 = \omega / c$ is the wave number. $N^2 = 1 - \omega_p^2 / \omega_c^2 = 1 - n_e / n_c$, $n_c = \omega^2 m \epsilon_0 / e^2$ is the critical density. If the plasma density is small enough, we then have $n_e / n_c (\omega_p^2 / \omega_c^2) \ll 1$. This condition is satisfied in our experiment. So the phase shift of the interference fringe is

$$\Delta\Phi = \frac{\omega}{c} \int \left[\left(1 - \frac{n_e}{n_c} \right)^{1/2} - 1 \right] dl \approx \frac{\omega}{2cn_c} \int n_e dl. \quad (3)$$

*Author to whom correspondence should be addressed. Email address: jzhang@aphy.iphy.ac.cn

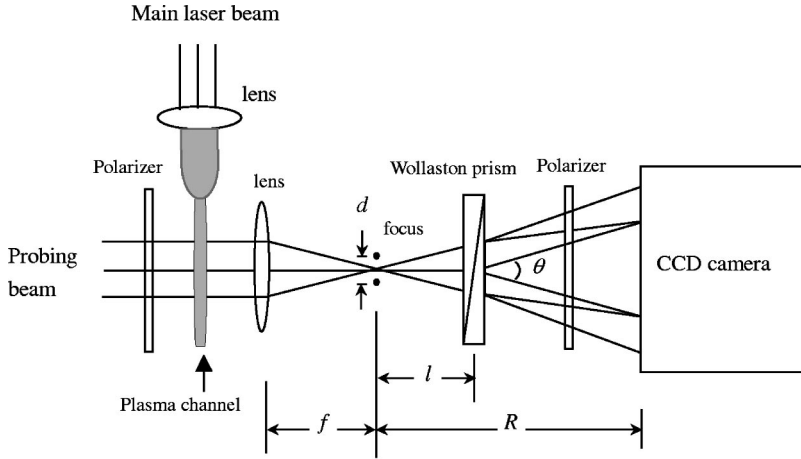


FIG. 1. Schematic of the experimental setup.

Assuming that the shift number is D , and $\Delta\Phi = 2\pi D$, then we have

$$\int n_e dl = 2Dn_c\lambda. \quad (4)$$

In this experiment, we are interested in the average electron density, so the expression (4) can be rewritten as

$$\bar{n}_e d = 2Dn_c\lambda, \quad (5)$$

where d is the diameter of the plasma channel. In the experiment, when the delay between the main laser and the probing beam is about 600 ps, the shift of the interference fringes was measured as shown in Figs. 3(a) and 3(b). The average shift number can be measured to be $\bar{D} = 1/8$. We can then obtain

$$\bar{n}_e = 2.7 \times 10^{18} \text{ cm}^{-3}. \quad (6)$$

The temporal history of the electron density was measured by the interferometric method as shown in Fig. 4. The

solid curve is the measured result and the dotted line is the fitting curve by the following expression:

$$n_e = 6.18 \times 10^{18} \exp^{-t/0.684}. \quad (7)$$

We can estimate the lifetime of the plasma channel from this result. After the plasma channel is formed, dynamics of the channel will follow the equation of continuity as follows [10,11]:

$$\frac{\partial n_e}{\partial t} + \frac{\partial V n_e}{\partial z} = \alpha n_e - \eta n_e - \beta_{ep} n_e n_{pn}. \quad (8)$$

$$\frac{\partial n_p}{\partial t} + \frac{\partial V n_p}{\partial z} = \alpha n_e - \beta_{ep} n_e n_{pn} - \beta_{np} n_n n_p, \quad (9)$$

$$\frac{\partial n_n}{\partial t} + \frac{\partial V n_n}{\partial z} = \eta n_e - \beta_{np} n_n n_p. \quad (10)$$

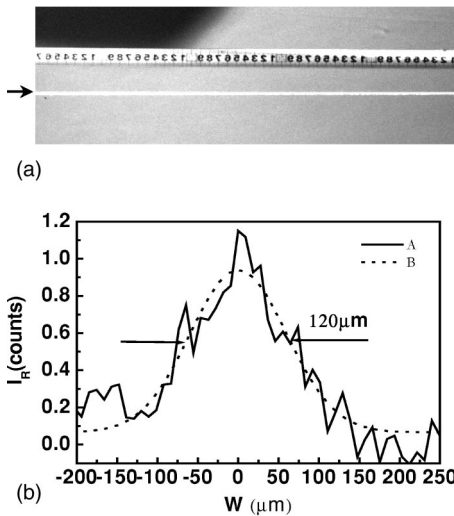
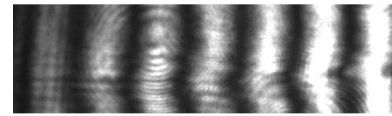
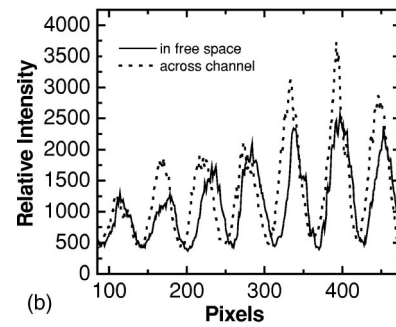


FIG. 2. (a) The image of a part of the plasma channel formed by a femtosecond laser beam with an $f=2$ m lens. (b) The relative intensity (I_R) distribution in the channel fitted by a Gaussian function (dotted curve).



(a)



(b)

FIG. 3. (a) The image of the interferometric fringes by a CCD camera. (b) The average shift in every interferometric fringe. The dotted curve represents the probing beam traversed the plasma channel, and the solid curve represents the probing beam in free space.

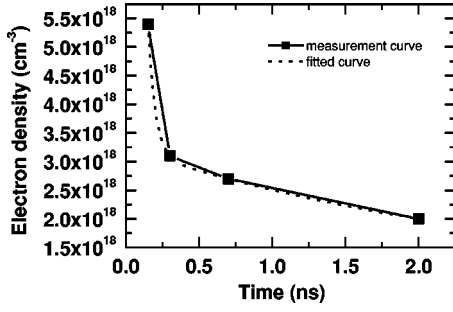


FIG. 4. The decay of the electron density in the plasma channel versus time.

where n_e, n_p, n_n are electron density, positive ions, and negative ions in air, respectively, as reported in Refs. [7,8], and $\alpha, \eta, \beta_{ep}, \beta_{np}$ are the collisional ionization rate, the attachment rate, the electron-ion recombination coefficient, and the ion-ion recombination coefficient, respectively. Assuming that the plasma density in the channel is uniform in space and neglecting the collisional ionization rate, we take $\eta = 2.5 \times 10^7 \text{ s}^{-1}$ for the attachment rate of electrons to oxygen, $\beta_{ep} = 2.2 \times 10^{-13} \text{ m}^3/\text{s}$ for the electron-ion recombination, and $\beta_{np} = 2.2 \times 10^{-13} \text{ m}^3/\text{s}$ for ion-ion recombination. Taking the following initial conditions,

$$n_e(t=0) = n_p(t=0) = 10^{18} \text{ cm}^{-3}, \quad n_n(t=0) = 0,$$

we can then obtain temporal evolution of the electron density in the channel as shown by curve *a* in Fig. 5, and find that the electron density decays three orders within 30 ns from curve *a*. In Fig. 5, the dashed curve *c* is an exponential decay fitting. So from curve *a* and *c* in Fig. 5, we can find that in the initial period, the electron density follows an exponential decay as we measured shown in Fig. 4. But at the longer time, the decay of the electron will deviate from the exponential decay. In many applications such as triggered lightning, plasma channels with longer lifetime are required. Usually, the plasma lifetime is constrained by the strong attachment of electrons to oxygen molecules to form negative ions O^- and O_2^- in air [11]. In order to maintain a high electron density in plasma channel, another long laser pulse is launched along the plasma channel, with an intensity I_2 to detach electrons from O^- and O_2^- . So we add another term $\gamma_l n_n$ in Eqs. (8)–(10), where γ_l is the detachment coefficient. For simplicity we can set the detachment rate η to be equal to the attachment rate, and the required intensity $I_2 = 6.8 \times 10^5 \text{ W/cm}^2$ was given by Ref. [11]. Then we can calculate the electron density in the plasma channel again, and find that the lifetime of the plasma is greatly prolonged, as shown by curve *b* in Fig. 5. The decay time for three orders is now greatly extended in the order of μs . This is an efficient way to extend the lifetime of plasma channel.

We measured the conductivity of the plasma channel using a similar method as described in Ref. [5]. Because the

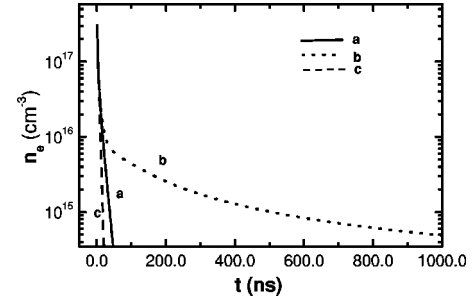


FIG. 5. The temporal dependence of the electron density in the channel. The solid curve *a* represents the free decay of the electron density in the channel, the dotted curve *b* represents the temporal evolution of the electron density in the plasma channels with a long-pulse laser after an femtosecond laser pulse. The dashed curve *c* represents the exponential decay fitting.

collisional frequency of electrons is about $1/\nu = 1.1 \text{ ps}$ in air, this is much shorter than the characteristic time for the evolution of an electron plasma. So we can treat it with a steady limit, which is Ohm's law. In our experiment, the parallel copper plates were separated by 6.5 cm. The electrical signals were recorded by a digital oscilloscope with a 500 MHz bandwidth (Tekex Corporation). A 8 k Ω resistance was used to limit the current and the signal voltage was obtained from a 50 Ω resistance by an oscilloscope. The signal voltage is shown in Fig. 4, when the applied voltage is 1500 V. The peak signal voltage across a 50 Ω resistance was 1580 mV. Following Ohm's law, we have

$$\eta = 0.76 \Omega \text{ cm}. \quad (11)$$

Because the connection between the plasma channel and the copper electrodes was not perfect, so the measured value is only the upper limit of the resistivity of the channel.

IV. CONCLUSIONS

Plasma channels over 5 m were observed when a femtosecond laser pulse propagated in air. The plasma lifetime can be greatly prolonged by launching another long laser pulse along the plasma channel. The size of the plasma channel was measured to be about 120 μm . Furthermore, the electron density in the plasma channel was measured to be about $n_e = 2.7 \times 10^{18} \text{ cm}^{-3}$ with an interferometric method and the resistivity of the plasma channel was less than 1 $\Omega \text{ cm}$, respectively. These experimental results are in good agreement with our theoretical analysis.

ACKNOWLEDGMENTS

We are thankful for the helpful discussion with Professor J. X. Ma. This work was supported by the National Natural Science Foundation of China (Nos. 19825110, 1000405, and 1997074) and National Key Basic Research Special Foundation (Grant No. G1990075200).

- [1] A. Braun, G. Korn, X. Liu, D. Du, J. Squier, and G. Mourou, *Opt. Lett.* **20**, 73 (1995).
- [2] E. T. J. Nibbering, P. E. Curley, G. Grillon, B. S. Prade, M. A. Franco, F. Salin, and A. Mysyrowicz, *Opt. Lett.* **21**, 62 (1996).
- [3] A. Brodeur, C. Y. Chien, A. Ilkov, S. L. Chin, O. G. Kosareva, and V. P. Kandidov, *Opt. Lett.* **22**, 304 (1997).
- [4] L. Wöste *et al.*, *Laser Optoelektron.* **5**, 29 (1997).
- [5] S. Tzortzakis, M. A. Franco, Y.-B. Andr, A. Chiron, B. Lamouroux, B. S. Prade, and A. Mysyrowicz, *Phys. Rev. E* **60**, R3505 (1999).
- [6] H. Yang, J. Zhang, W. Yu, Y. J. Li, and Z. Y. Wei, *Phys. Rev. E* **65**, 016406 (2002).
- [7] S. Tzortzakis, B. Prade, M. Franco, and A. Mysyrowicz, *Opt. Commun.* **181**, 123 (2000).
- [8] B. L. Fontaine, F. Vidal, D. Comtois, C. Y. Chien, A. Despa-rois, T. W. Johnston, J. C. Kieffer, H. P. Mercure, H. Pépin, and F. A. M. Rizk, *IEEE Trans. Plasma Sci.* **27**, 688 (1999).
- [9] H. Yang, J. Zhang, J. X. Ma, and W. Yu, *High Power Laser Particle Beams* **5**, 537 (2000), in Chinese.
- [10] L. B. Loeb, *Basic Processes of Gaseous Electronics* (University of California Press, Berkeley, 1960), p. 618.
- [11] X. M. Zhao, J. C. Diel, C. Y. Wang, and J. M. Elizondo, *IEEE J. Quantum Electron.* **31**, 599 (1995).
- [12] Y. T. Li *et al.*, *Sci. China, Ser. A Math., Phys., Astron.* **43**, 1249 (2000).